ORIGINAL RESEARCH

Macrophage Foam Cell–Derived Extracellular Vesicles Promote Vascular Smooth Muscle Cell Migration and Adhesion

Chenguang Niu, MD, PhD;* Xu Wang;* Mingming Zhao; Tanxi Cai, PhD; Peibin Liu, MS; Jizhao Li, MD, MS; Belinda Willard, PhD; Lingyun Zu, MD, PhD; Enchen Zhou, MS; Yufeng Li, MD, PhD; Bing Pan, PhD; Fuquan Yang, PhD; Lemin Zheng, PhD

Background—A new mechanism for intercellular communication has recently emerged that involves intercellular transfer of extracellular vesicles (EVs). Several studies have indicated that EVs may play a potential role in cell-to-cell communication between macrophage foam cells and vascular smooth muscle cells (VSMCs) in atherosclerotic lesion.

Methods and Results—This study involved the comparison of circulating EVs from atherosclerotic patients and control participants. The results showed that the circulation of the patients contained more leukocyte-derived EVs and that these EVs promoted more VSMC adhesion and migration than those of healthy participants. We then established a macrophage foam cell model and characterized the EVs from the macrophages. We used flow cytometric analyses and cell migration and adhesion assays and determined that the foam cells generated more EVs than the normal macrophages and that the foam cell–derived EVs were capable of promoting increased levels of VSMC migration and adhesion. Furthermore, we performed a proteomic analysis of the EVs. The data showed that the foam cell–derived EVs may promote VSMC adhesion and migration by regulating the actin cytoskeleton and focal adhesion pathways. In addition, Western blotting revealed that foam cell–derived EVs could promote the phosphorylation of ERK and Akt in VSMCs in a time-dependent manner. We also found that foam cell–derived EVs could enter the VSMCs and transfer integrins to the surface of these cells.

Conclusions—The data in our present study provide the first evidence that EVs from foam cells could promote VSMC migration and adhesion, which may be mediated by the integration of EVs into VSMCs and the subsequent downstream activation of ERK and Akt. **(*J Am Heart Assoc*. 2016;5:e004099 doi: 10.1161/JAHA.116.004099)**

Key Words: atherosclerosis • exosomes • microparticles • microvesicles • proteomics

Intercellular communication is a critical function in all multicellular organisms. Cells exchange information through the secretion of soluble factors or by direct interaction. In recent years, a new mechanism for intercellular communication has emerged that involves intercellular transfer of extracellular vesicles (EVs). EVs are phospholipid bilayer membrane-enclosed vesicles that are 30 to 2000 nm in diameter; that contain proteins, lipids, and nucleic acids; and that are released to the extracellular space by various types of cells.[1–6] Based on their biogenesis, EVs are classified as exosomes, microvesicles, or apoptotic bodies. Because apoptotic bodies have been long known and well studied, the current interest in the field is focused primarily on the first 2 classes of EVs. Exosomes are generated by exocytosis of multivesicular bodies and are 30 to 100 nm in diameter,[7] whereas microvesicles (50–1000 nm in diameter)—also known as microparticles, ectosomes, or shedding vesicles—are generated by budding

From the Institute of Cardiovascular Sciences and Institute of Systems Biomedicine, School of Basic Medical Sciences (C.N., X.W., M.Z., J.L., E.Z., B.P., L.Z.) and Key Laboratory of Molecular Cardiovascular Sciences of Ministry of Education (C.N., X.W., M.Z., J.L., E.Z., B.P., L.Z.), Peking University Health Science Center, Beijing, China; Laboratory of Protein and Peptide Pharmaceuticals and Laboratory of Proteomics, Institute of Biophysics, Chinese Academy of Sciences, Beijing, China (T.C., P.L., F.Y.); Proteomics Laboratory, Cleveland Clinic, Cleveland, OH (B.W.); Department of Cardiology, Peking University Third Hospital, Beijing, China (L.Z.); Department of Endocrinology and Metabolism, Capital Medical University Pinggu Teaching Hospital, Beijing, China (Y.L.).

Accompanying Figures S1 through S4 and Table S1 are available at http://jaha.ahajournals.org/content/5/10/e004099/DC1/embed/inline-supplementary-material-1.pdf

*Dr Niu and Dr Wang contributed equally to this work.

Correspondence to: Fuquan Yang, PhD, Institute of Biophysics, Chinese Academy of Sciences, Beijing 100101, China. E-mail: fqyang@ibp.ac.cn
Lemin Zheng, PhD, Institute of Cardiovascular Sciences, Peking University Health Science Center, Beijing 100191, China. E-mail: zhengl@bjmu.edu.cn

Received June 23, 2016; accepted September 13, 2016.

from the plasma membrane and are generally larger than exosomes.[2,8,9]

EVs were initially regarded as membrane debris with no real biological significance. In 1996, however, Raposo et al showed that EVs could stimulate immune responses.[10] Since then, the importance of EVs in intercellular communication has been confirmed in numerous studies.[4,8,11–13] It has become increasingly evident that these vesicles play key roles not only in the regulation of normal physiological processes, including stem cell maintenance, tissue repair, immune surveillance, and blood coagulation but also in the pathology underlying several diseases.[10,14–16] EVs have been implicated in the stimulation of tumor progression through their abilities to stimulate tumor growth and angiogenesis, to promote matrix remodeling, to induce metastasis, and to promote immune escape by modulating T-cell activity.[4,17,18] In addition, EVs have been proposed to play roles in neurodegenerative diseases by transporting prions, β-amyloid peptide, and α-synuclein.[19–21] Moreover, the roles of EVs in cardiovascular disease have been described and have attracted increasing attention in recent years.[22–25]

Cardiovascular disease is the leading cause of death in humans and accounts for ≈30% of all deaths in the United States. Atherosclerosis is a primary cause of cardiovascular disease.[26] Atherosclerosis is a progressive disease characterized by the accumulation of lipids and fibrous elements in large arteries. The early lesions of atherosclerosis, which are called *fatty streak lesions*, consist of subendothelial accumulations of cholesterol-engorged macrophages called *foam cells*. These initial lesions are followed by fibrous lesions, which are characterized by the accumulation of lipid-rich necrotic debris and vascular smooth muscle cells (VSMCs).[27] Studies of the pathogenesis of this disease over the past 50 years have revealed that numerous cellular and molecular mechanisms are involved in atherogenesis and that foam cells play a key role. A series of findings have revealed that cytokines secreted by foam cells are important for VSMC proliferation and migration into the intima and for extracellular matrix production, in that matrix production is responsible for the formation of fibrous plaques. Nevertheless, the forms of communication between macrophage-derived foam cells and VSMCs have not been fully defined.

A number of studies recently indicated that cardiovascular system–related cells, including platelets, erythrocytes, endothelial cells, leukocytes, monocytes, macrophages, and smooth muscle cells, release EVs that play biological and/or pathological roles in cardiovascular disease.[28–30] Interestingly, we found that circulating EVs from atherosclerotic patients could promote more VSMC adhesion and migration than those from healthy participants. Moreover, we found that macrophage-derived foam cells released a higher number of EVs than normal macrophages. Because EVs mediate intercellular communication, we proposed that intimal foam cells may modulate the function of VSMCs via EVs during the progression of atherosclerosis. In this study, we extensively assessed the effects of foam cell–derived EVs (FC-EVs) on VSMC adhesion and migration.

Materials and Methods

Participants

This study included 25 healthy participants and 25 patients with atherosclerosis. The patients met Chinese diagnostic criteria for coronary atherosclerotic heart disease (health standard WS 319-2010), and all diagnoses were confirmed by coronary angiography. Patients with diabetes mellitus or cerebral hemorrhage were excluded from this study to eliminate interference on the basis that circulating EVs from these patients are considered to be abnormal.[31,32] The patients were matched with healthy participants of the same age and sex. The healthy participants underwent relevant examinations to exclude cardiovascular diseases and diabetes mellitus. In addition to this group, 5 healthy participants were recruited for the isolation of low-density lipoprotein (LDL). Written informed consent was provided by every participant before the study began, and the local ethics committee approved the protocol for this study. General information on the participants enrolled in this study is shown in Table 1.

Cell Culture

The J774a.1, THP-1, and U937 macrophage cell lines were purchased from the Cell Resource Center, Chinese Academy of Medical Sciences (Beijing, China). Human aortic VSMCs were purchased from Shanghai Xinyu Biological Technology Co., Ltd. (Shanghai, China). VSMCs between passages 3 and 6 were used for our experiments. The J774a.1 cells and VSMCs were cultured in DMEM (10-013-CVR; Corning) containing 10% FBS (10099141; Gibco) and were cultured at 37°C in an incubator (Sanyo) with a humidified atmosphere containing 5% carbon dioxide.

Oxidized LDL and Foam Cell Formation

Fresh fasting plasma was separated by centrifugation from the peripheral blood obtained from healthy participants and mixed together. LDL was isolated from plasma by density gradient ultracentrifugation and then oxidized using 5 μmol/L copper sulfate. The oxidized LDL was dialyzed 3 times against 1 L of PBS (10 mmol/L, pH 7.0), sterilized with a 0.22-μm filter, stored in sealed tubes at 4°C in the dark, and used within 2 months. The level of sample oxidation was measured using the thiobarbituric acid method, and its value was

Table 1. Participant Characteristics

Characteristics	Healthy (n=25)	Atherosclerotic (n=25)	*P* Value
Sex (female), %	56	44	0.5716
Age, y	62.76±1.73 (62)	63.64±2.20 (65)	0.7549
Smoking, %	44	52	0.7771
Triglycerides, mmol/L	1.61±0.13 (1.41)	1.47±0.15 (1.27)	0.4792
TC, mmol/L	4.59±0.22 (4.71)	4.10±0.20 (3.96)	0.1075
LDL-C, mmol/L	1.16±0.05 (1.14)	1.03±0.06 (1.02)	0.1155
HDL-C, mmol/L	2.78±0.18 (2.96)	2.50±0.18 (2.31)	0.2642
Hyperlipidemia, %	44	44	1
Lipid-lowering medication, %	24	40	0.5601
Hypertension, %	64	76	0.5371
Antihypertensive medication, %	44	44	1
Diabetes mellitus, %	0	0	—
Intracerebral hemorrhage, %	0	0	—
Myocardial infarction, %	0	36	0.0032

Scale values are described as mean±SD (median), whereas nominal values are described as percentages. HDL-C indicates high-density lipoprotein cholesterol; LDL-C, low-density lipoprotein cholesterol; TC, total cholesterol.

9.2 nmol of malondialdehyde equivalents per milligram of LDL. Formation of foam cells from J774a.1 cells was initiated by treating 50% confluent cultures of these cells with DMEM containing 50 μg/mL oxidized LDL for 24 hours. Parallel 50%-confluent J774a.1 cultures treated for 24 hours with DMEM containing no oxidized LDL were used as a control. Oil Red O staining was used to determine the quality of foam cell formation.

EV Isolation

Circulating EVs were isolated, as described previously.[33] Briefly, 2 to 3 mL of blood was collected from participants and immediately centrifuged at 1000*g* for 15 minutes at 4°C and subsequently at 15 000*g* for 3 minutes to obtain platelet-free plasma. The platelet-free plasma was ultracentrifuged at 100 000*g* (4°C, 1 hour) to pellet the EVs. The EVs were then resuspended in a volume of DMEM equal to the original plasma volume. EVs from the in vitro cultures were isolated as follows. The culture media from J774a.1 cells and the J774a.1-derived foam cells were collected and centrifuged at 300*g* for 5 minutes and subsequently at 500*g* for 5 minutes to remove cell debris. Next, the medium was ultracentrifuged at 100 000*g* at 4°C for 1 hour. After that, the EV pellets were resuspended in DMEM in the same volume as the collected culture media or another medium at the indicated volume. The protein concentrations of the EV preparations were quantified using a MicroBCA Protein Assay Kit (Thermo Scientific). Both circulating and in vitro EVs were stored at 4°C and used to treat cells or to perform other experiments within 48 hours. All steps for isolation of the EVs that were to be used for cell treatments were performed using sterile techniques.

Wound-Healing Assay

VSMCs were plated in 6-well plates using DMEM containing 10% FBS and cultured until cell monolayers formed. Monolayers were wounded by manual scraping with a 10-μL micropipette tip and then washed. The cells were then incubated with medium containing 1% FBS alone or combined with the indicated concentrations of circulating or cell-derived EVs or other treatment factors for 36 hours. The cells were fixed with methanol, stained with crystal violet, and photographed using an inverted microscope. The cells that migrated past the wound edge were quantified in 3 high-power fields (left field, middle field, and right field).

Cell-Adhesion Assay

Cell adhesion was measured using the MTT assay, as described previously.[34] Briefly, 96-well plates were coated with 2 μg per well of basement membrane matrix (Matrigel; BD Biosciences) for 1 hour at 37°C and then blocked with 2% bovine serum albumin for 2 hours at 37°C, followed by washing twice. VSMCs were seeded on 6-well plates and then treated with serum-free DMEM alone or combined with EVs or other treatment factors for 6 hours. After detachment with

trypsin, cells (5×10^3 per well) were plated on Matrigel-precoated 96-well plates, and after 45 minutes, the wells were washed twice with PBS to remove nonadherent cells. MTT colorimetric assays were conducted, and the absorbance at 570 nm was measured to quantify adherent cells. Five parallel wells were set up for each condition.

Flow Cytometry

A volume of 50 μL of platelet-free plasma or debris-free cell culture medium was collected for flow cytometric analysis. The sample was added to a mixture of fluorescent stains (4 μL each) and 200 μL of binding buffer. For plasma samples, 4 μL of heparin was added. The mixtures were incubated in the dark at room temperature for 30 minutes and then transferred into Trucount tubes (BD Biosciences) for measurement using a Gallios flow cytometer (Beckman Coulter).

The gate determination for EVs was based on the use of calibrated fluorescent beads (Megamix beads; BioCytex).[35] The EV analysis region was defined as follows: The lower side was defined by the threshold allowing the acquisition of events of at least 0.5 μm, and the upper side was the end of the 0.9-μm bead cloud. On the 10-base logarithm value of side light scatter by 10-base logarithm value of forward light scatter dot plot, an EV auto gate with a maximum sensitivity of ≈0.9 μm was created. The EV gate can be seen in our previous work.[36] Characterization of the EVs was performed through fluorescently labeled annexin V (annexin V-APC [allophycocyanin]; KeyGen Biotech) and a CD45 antibody (anti–CD45-PerCP/Cy5.5; BioLegend).[37] The FL6 photomultiplier tube was set to detect the fluorescence emitted by annexin V-APC, and FL4 was set to detect the fluorescence emitted by anti–CD45-PerCP/Cy5.5. An untreated sample and a sample treated with isotypic immunoglobulin G were used to define EVs positive for exposed phosphatidylserine (PS) and CD45, respectively. Quantitative determination of EVs was performed using Trucount beads. We set the FL1 and FL4 photomultiplier tubes to identify the Trucount beads, and the proportion of sample flowing into Gallios was calculated by counting the detected Trucount beads. The total EV numbers in the tube were determined using the following formula:

$$\text{Total EV numbers} = \text{Detected EV numbers} \times \frac{\text{Total Trucout Bead Numbers in Tube}}{\text{Detected Trucout Bead Numbers}}$$

Electron Microscopy and Dynamic Light Scattering

A volume of 1 mL of debris-free conditioned medium from the J774a.1-derived foam cell cultures was prepared for electron microscopy. The sample was negatively stained with 2% phosphotungstic acid, placed onto a carbon-coated perforated film supported by a copper grid, and examined using a JEM-1400 plus transmission electron microscope (JEOL) at 100 kV.

Dynamic light scattering analysis of the EVs was performed using a Delsa Nano C particle analyzer (Beckman Coulter). Briefly, a volume of 1 mL of debris-free medium from the J774a.1-derived foam cell cultures was transferred into a cuvette, placed in the analyzer, and evaluated twice.

Proteome Analysis

The EV samples were prepared using the FASP (Filter Aided Sample Preparation) protocol for mass spectrometry. Two technical replicates were analyzed. The analyses were performed using a nano– liquid chromatography LTQ Orbitrap XL mass spectrometer (Thermo Scientific) at a resolution of 60 000. The raw data were processed using Proteome Discoverer (version 1.4.0.288; Thermo Scientific). The tandem mass spectra were searched with the SEQUEST search engine against the Uniprot mouse complete proteome database (release 2014_06, 50 790 protein sequences). The peptide spectral matches were validated using a targeted decoy database search at a 1% false discovery rate. The identified peptides were grouped into proteins according to the law of parsimony. The identified proteins were quantified using the sum of the spectral counting of the 3 most intense parent ions of the corresponding peptide. KEGG (Kyoto Encyclopedia of Genes and Genomes) pathway analysis of the EV proteome was performed using the Database for Annotation, Visualization, and Integrated Discovery (DAVID v6.7).

Confocal Laser Scanning Microscopy

The J774a.1 cells were labeled with a 20-μmol/L CellTracker fluorescent probe (green fluorescence; Life Technologies) for 30 minutes prior to treatment with oxidized LDL for foam cell formation. EVs were then isolated from the CellTracker-labeled foam cells and used to treat VSMCs for 1 hour. VSMCs were washed twice, fixed for 10 minutes, stained with DiI (red fluorescence to label the lipid membranes) and DAPI (blue fluorescence to label the nuclei), and prepared for confocal laser scanning microscopic imaging.

Cell Enzyme-Linked Immunosorbent Assay

VSMCs were placed in 96-well plates and grown to 80% confluence and then treated with FBS-free medium containing 20 μg/mL of FC-EVs for 0 minutes, 15 minutes, 30 minutes, 1 hour, or 2 hours. The cells were washed with PBS and fixed with methanol for 5 minutes and then washed 3 times with PBS and blocked with 2% bovine serum albumin for 2 hours at

37°C. The integrins on the cell surfaces were evaluated using primary monoclonal antibodies for integrin β1 (ab52971; Abcam) or integrin α5 (ab150361; Abcam), followed by binding of an HRP-conjugated secondary antibody (1:2000). The bound antibodies were quantified using a TMB peroxidase EIA substrate kit (Thermo Scientific), and the intensity of the color developed at an optical density at 450 nm was evaluated. Five parallel wells were set up for each condition.

Real-Time Polymerase Chain Reaction

VSMCs were placed in 6-well plates and grown to 80% confluence and then treated with FBS-free medium containing 20 μg/mL of FC-EVs for 0 minutes, 15 minutes, 30 minutes, 1 hour, or 2 hours. The total RNA was extracted from VSMCs using TRIzol (Thermo Scientific), and first-strand cDNA was prepared using the TransScript RT enzyme (TransGen Biotech). Primer sets specific for integrin β1, integrin α5, and GAPDH were used to direct the polymerase chain reaction (94°C for 5 minutes and 40 cycles of 94°C for 30 seconds, 60°C for 30 seconds, and 72°C for 30 seconds, and then 72°C for 5 minutes). The linear expression range of each gene was determined by serial dilutions of each cDNA pool and normalized to the expression of GAPDH. The forward and reverse primer sequences were as follows: CAAGAGAGCTGAAGACTATCCCA and TGAAGTCCGAAGTAATCCTCCT for integrin β1, GCCTGTGGAGTACAAGTCCTT and AATTCGGGTGAAGTTATCTGTGG for integrin α5, and GGAGCGAGATCCCTCCAAAAT and GGCTGTTGTCATACTTCTCATGG for GAPDH.

Western Blot

The samples were lysed using RIPA buffer in the presence of protease inhibitors and phosphatase inhibitors. The lysates (30 μg proteins per lane) were subjected to electrophoresis on 10% SDS polyacrylamide gels and transferred to nitrocellulose membranes according to standard procedures. The membranes were blocked for 1 hour and incubated with the primary antibody overnight at 4°C, followed by incubation with the corresponding HRP-conjugated secondary antibody for 1 hour. Antibody binding was detected using a Pierce Super Signal West Pico Kit (Thermo Scientific). All antibodies were diluted according to the manufacturers' protocols. The sources of the primary antibodies were as follows: anti–total ERK (ab17942; Abcam), anti–phosphorylated ERK (ab4819; Abcam), anti–total Akt (4691; Cell Signaling Technology), and anti–phosphorylated Akt (2965; Cell Signaling Technology).

Statistics

GraphPad Prism 6 (GraphPad Software) was used for statistical analysis. Data distributions were tested for normality using the Shapiro–Wilk test. If the data distribution passed normality tests, 1-way ANOVA was used for multiple comparisons, with the Tukey test for post hoc testing (data presented as mean±SEM). If the data distribution failed normality tests, the Wilcoxon rank sum test was used to determine *P* values for single comparisons, or a Kruskal–Wallis test was applied with a Dunn multiple comparisons test for significant *P* values (data presented as median with 25th and 75th percentiles). The differences were considered significant at $P<0.05$. All biological results were confirmed by at least 3 independent experiments.

Results

Atherosclerotic Circulating EVs Are More Capable of Promoting VSMC Adhesion and Migration

EVs were isolated from plasma samples of the healthy and atherosclerotic participants, resuspended in a volume of DMEM equal to the original plasma volume, and used to treat cells to study the biological functions of EVs. Wound-healing and adhesion experiments were performed to assay the effect of EVs on the migration and adhesion of VSMCs. As shown in Figure 1A and 1B, circulating EVs from the atherosclerotic patients promoted VSMC migration, with a 28.6% increase compared with EVs from healthy participants. Figure 1C shows similar results with respect to the capacity of circulating EVs from atherosclerotic patients to promote VSMC adhesion: A 15.9% increase was observed compared with EVs from healthy participants.

Atherosclerotic Plasma Contains More Leukocyte-Derived EVs

We developed a Trucount tube–based flow cytometry method to detect and quantify circulating EVs. Because exposed PS is a marker of EVs, we identified EVs by labeling with annexin V. It is known that circulating EVs originate from multiple sources and that they carry some markers of the cells of origin. On the basis that atherosclerosis is a progressive chronic inflammatory disease,[38] we focused our interest on leukocyte-, monocyte-, and macrophage-derived EVs and identified them by labeling with CD45.

In this study, we chose 10 healthy participants and 10 atherosclerotic patients for the flow cytometric analysis. Figure 1D through 1F displays the results and shows that the numbers of PS- and CD45-positive EVs from atherosclerotic patients were both significantly greater than those from healthy participants. The mean numbers of PS- and CD45-positive EVs from atherosclerotic participants were 6552.1/μL and 1409.2/μL, respectively, whereas those from the healthy participants were 2945.5/μL and 765.7/μL, respectively.

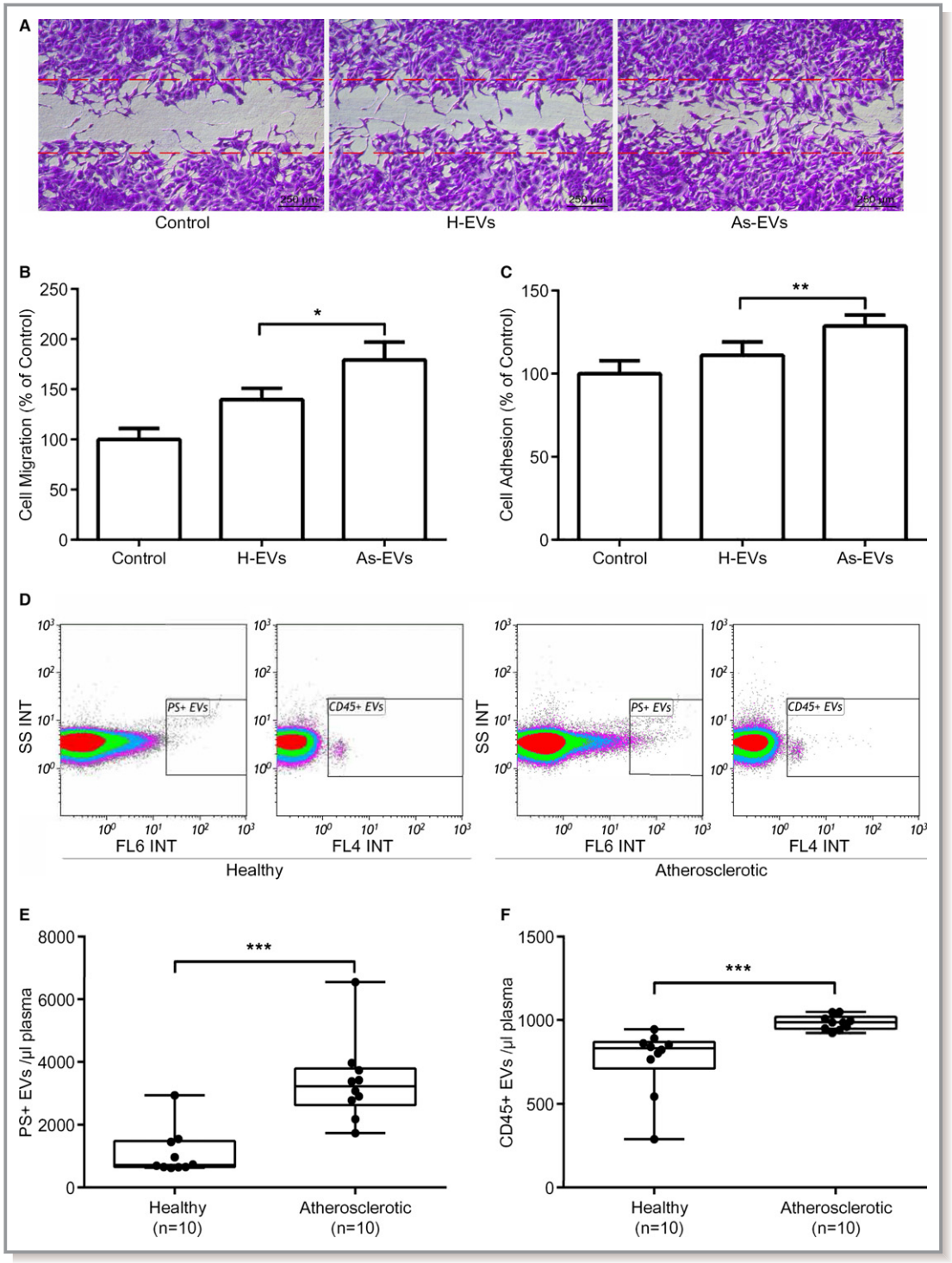

Figure 1. As-EVs promote VSMC adhesion and migration. A through C, The data for the wound-healing and cell-adhesion assays in VSMCs after the indicated treatments. A, A representative photograph of VSMC migration in the wound-healing assay. B, The quantitative results for VSMC migration. C, The results of the VSMC-adhesion experiments. D through F, The data for the flow cytometric analysis of circulating EVs. Ten healthy participants and 10 atherosclerotic patients were included. D, Representative density plots of exposed PS- and CD45-positive EVs from the plasma of the healthy and atherosclerotic participants. E and F, The statistical results for PS- and CD45-positive EVs, respectively. Because the data distribution failed to pass normality tests, the Wilcoxon rank sum test was used to determine *P* values. **P*<0.05, ***P*<0.01, ****P*<0.001. As-EVs indicates circulating extracellular vesicles from atherosclerotic participants; EV, extracellular vesicle; H-EVs, circulating extracellular vesicles from healthy participants; SS, side light scatter; INT, intensity; PS, phosphatidylserine; VSMC, vascular smooth muscle cell.

J774a.1-Derived Foam Cells Release More EVs

There is currently no effective way to isolate leukocyte-, monocyte-, and macrophage-derived EVs from a pool of EVs obtained from an in vivo source. Alternatively, we chose a classical foam cell formation model that mimicked macrophage-derived EVs in atherosclerosis. After treatment with 50 μg/mL of oxidized LDL for 24 hours, J774a.1 macrophages transformed to foam cells. This is shown by the Oil Red O staining in Figure 2A; this stain binds to fatty acids.

To confirm EV production by foam cells, we conducted a transmission electron microscopic analysis. As shown in Figure 2B, several elliptical EVs of 50 to 100 nm in diameter were identified in the supernatants of foam cells, consistent with previous studies.[39] Next, we performed a dynamic light scattering analysis to determine the distribution of diameters within the EV population. As shown in Figure 2C, the sizes of FC-EVs ranged from tens to hundreds of nanometers in diameter, and the peak value of the diameter distribution was 67.6 nm, whereas normal macrophage–derived EVs (NM-EVs) were similar to FC-EVs. Previous studies have reported that integrins are main components of EVs.[40] We used Western blotting analyses to confirm that, in our study, membrane proteins including both integrins β1 and α5 were enriched in FC-EVs and NM-EVs. These proteins were absent in the EV-depleted culture media after ultracentrifugation for the isolation of EVs (shown in Figure 2D), which proved the validity of methods for isolating EVs in this study.

We quantified the EVs produced by foam cells and normal macrophages by flow cytometry. As shown in Figure 2E through 2G, macrophage-derived foam cells released more EVs than normal macrophages. Specifically, PS-positive EVs were increased by nearly 500% and CD45-positive EVs were increased by 33.5%. The mean numbers of PS- and CD45-positive EVs from foam cells were 2774.5 and 1398.6 per 1000 cells, respectively, whereas the numbers of PS- and CD45-positive EVs from normal macrophages were 468.6 and 1048.7 per 1000 cells, respectively. Next, we isolated EVs from the media and used the MicroBCA Protein Assay Kit to determine the total protein content of the suspension, which was then normalized to the number of cells. As shown in Figure 2H, foam cells and normal macrophages contributed 126.4 and 50.7 μg of EV protein per million cells, respectively, corresponding to a 2.5-fold difference.

FC-EVs Promote VSMC Adhesion and Migration

To investigate the effects of macrophage-derived EVs on VSMC migration and adhesion, we isolated EVs from the culture media of normal J774a.1 cells and J774a.1 foam cells and treated VSMCs with isolated EVs in wound-healing and cell-adhesion experiments. The results showed that FC-EVs markedly promoted VSMC migration and adhesion, with increases of 44.6% and 18.6%, respectively, relative to the control, whereas NM-EVs had neither of these effects (Figure 3A through 3C). In the wound-healing experiments (Figure 3A and 3B), FC-EVs promoted VSMC migration 39.7% more than NM-EVs. The results from the adhesion assay were similar. As seen in Figure 3C, FC-EVs promoted VSMC adhesion 18.7% more than NM-EVs. We also confirmed these experiments using THP-1 and U937 cell models (Figures S1 and S2). We also found that FC-EVs promoted endothelial cell migration and adhesion (Figure S3).

It is well known that a large number of soluble molecules in culture media may influence VSMC behavior. Unfortunately, there is no perfect method to isolate EVs from media without incorporating any soluble molecules. To eliminate the interference of the soluble molecules contained in EV preparations, we treated VSMCs with the foam cell culture media and EV-depleted culture media (foam cell culture media without EVs) in the migration and adhesion experiments. As shown in Figure 3A through 3C, removal of EVs from the media resulted in significant decreases in the capability of the foam cell culture media to promote VSMC migration (28.7% decrease) and adhesion (17.9% decrease).

The experiments described used NM-EVs and FC-EVs that were released from the same number of cells, isolated from the same volume of culture media, and resuspended in the same volume of DMEM. The number of EVs produced by foam cells, however, is not the same as that produced by normal macrophages. The protein concentration of NM-EVs in the culture media used to treat VSMCs was much less than that of FC-EVs. To determine whether the differences observed in the promotion of VSMC migration and adhesion were caused by differences in protein concentration, additional experiments were performed in which VSMCs were treated with NM-EVs that had been resuspended in DMEM to a 0.4-fold volume of the culture media and that had a concentration (20 μg/mL) ≈2.5-fold higher than the previous treatment concentration (8 μg/mL) and the same as that contributed by FC-EVs (20 μg/mL). As shown in Figure 3D through 3F, there were no obvious differences between the groups treated with 8 and 20 μg/mL NM-EVs in either the wound-healing or cell-adhesion experiments. Nevertheless, experiments performed with FC-EVs at the concentration equivalent to that of the NM-EVs showed that FC-EVs had higher migration and adhesion-enhancing effects on VSMCs.

Proteomics Analysis of FC-EVs

The reported data show that FC-EVs have significantly different effects on VSMCs than an equivalent amount of NM-EVs. These results implied that the contents of FC-EVs

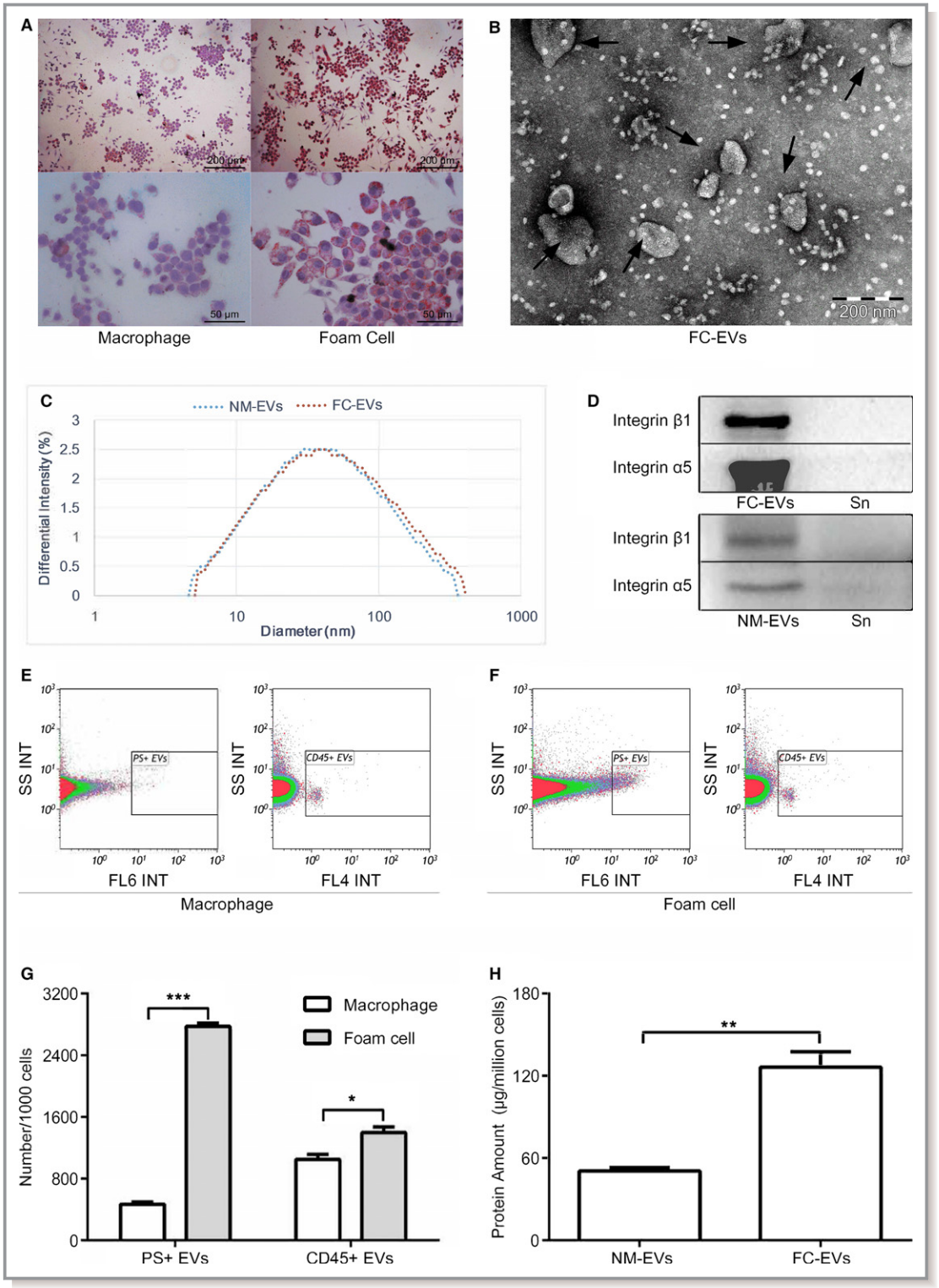

Figure 2. Foam cells release more EVs. A, The morphology of J774a.1-derived macrophages and foam cells stained with Oil Red O. B, An electron microscopic image of the FC-EVs. C, The distribution of the EV diameters as indicated by dynamic light scattering analysis. D, Western blot analysis for the EVs and EV-depleted supernatant. E and F, Representative density plots of the flow cytometric analysis of PS- and CD45-positive NM-EVs and FC-EVs. G, Quantification of the numbers of PS- and CD45-positive EVs. H, The result of the quantitative protein analysis of NM-EVs and FC-EVs. **P*<0.05, ***P*<0.01, ****P*<0.001. EV indicates extracellular vesicle; FC-EVs, foam cell–derived extracellular vesicles; NM-EVs, normal macrophage–derived extracellular vesicles; Sn, centrifugal supernatant for EVs; SS, side light scatter; INT, intensity; PS, phosphatidylserine.

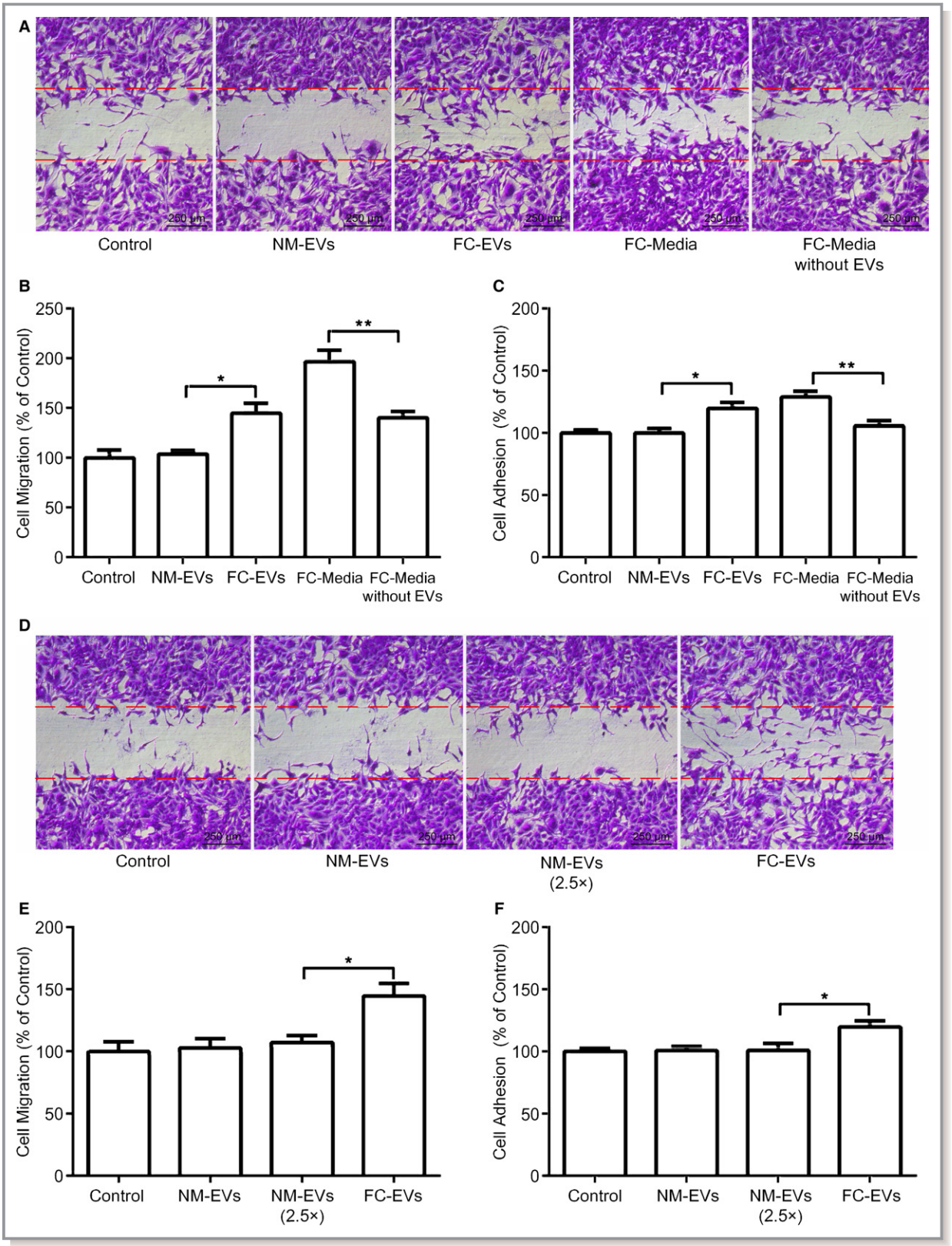

Figure 3. FC-EVs promote VSMC adhesion and migration. NM-EVs (2.5×) indicates that VSMCs were treated with NM-EVs with a concentration 2.5-fold as high as the NM-EV group. A and D, Representative photographs of VSMC migration in the wound-healing assay. B and E, Quantitative results of VSMC migration. C and F, Results of the VSMC-adhesion experiments. *P<0.05, **P<0.01. EV indicates extracellular vesicle; FC-EVs, foam cell–derived extracellular vesicles; FC-Media, foam cell culture media; NM-EVs, normal macrophage–derived extracellular vesicles; VSMC, vascular smooth muscle cell.

may differ from those of NM-EVs. Consequently, we performed a proteomic experiment to define the protein profile of FC-EVs. The proteomic experiments were performed on 2 FC-EV and 2 NM-EV samples analyzed in duplicate using nano–liquid chromatography and tandem mass spectrometry.

The proteomic experiments identified 599 proteins, with 203 and 571 proteins being detected in FC-EVs and NM-EVs, respectively (Figure 4A and Table S1). A *t* test analysis showed that there were 269 significant differentially expressed proteins between the 2 groups of EVs in which most of the differences in FC-EVs resulted from increased expression (Figure 4B). We then conducted a KEGG pathway analysis for these differentially expressed proteins. An exciting result was that the data showed these proteins may act on VSMCs via the "actin cytoskeleton regulation" and "focal adhesion" pathways, which agreed with our data on the ability of FC-EVs to promote VSMC adhesion and migration. The differentially expressed proteins involved in these pathways are marked in Figure 4C and 4D and listed in Table 2.

Interestingly, the proteomic data showed that numerous EV markers were contained in FC-EVs. These markers included tetraspanin CD9, VAMP8, HSP7C, HSP90B, HSP90A, HSP60, HSP10, HSP70-13, HSP70-4, PCD6IP, MFGE8, LAMP1, integrin β1, integrin α5, integrin αM, and integrin β2. The proteomic analysis also showed some monocyte and macrophage markers, including CD14 and CD45.

FC-EVs Activate the ERK and Akt Pathways

The reported data indicated that FC-EVs contained numerous proteins that are involved in cell migration and adhesion pathways and that these EVs could promote VSMC migration and adhesion. It is well known that some key downstream signaling molecules, including ERK and Akt, are involved in cell migration and adhesion. Consequently, the phosphorylation levels of these molecules may change during FC-EV–induced promotion of VSMC migration and adhesion. To evaluate this possibility, we treated 80%-confluent VSMCs with 20 μg/mL of FC-EVs and then determined the total and phosphorylated levels of ERK and Akt in the cells using Western blotting. As expected, treatment with EVs resulted in time-dependent increases in the phosphorylation of ERK and Akt in VSMCs. At 4 hours, when the highest level of activation was observed, the phosphorylation of these proteins was increased by 47.0% and 55.7%, respectively (Figure 5A and 5B); however, the NM-EVs had no effect on these pathways (Figure 5C and 5D).

FC-EVs Transport Proteins Into VSMCs

To determine whether FC-EVs could enter and release their contents into VSMCs to further affect cell functions, we labeled FC-EVs using the CellTracker fluorescent probe (green). This probe can freely pass through cell membranes and contains a chloromethyl group that reacts with thiol groups via a glutathione S-transferase–mediated reaction. After the reaction, the probe is retained well in living cells through several generations and thus was retained in EVs that were released by the probe-labeled cells. VSMCs were treated with the CellTracker-labeled EVs for 1 hour, washed, and stained with the additional fluorescent dyes DiI (red) and DAPI (blue). Figure 6A shows some green EVs scattered in these cells.

The Western blot analysis (Figure 2D) and proteomics data (Table 1) described above showed that integrins β1 and α5 are contained in FC-EVs. In this study, we chose these 2 proteins to verify that EVs transport proteins into VSMCs. On the basis that integrins are membrane proteins, we conducted a cell enzyme-linked immunosorbent assay experiment to survey the progression of the transport of integrins from EVs to VSMCs. After treatment with FC-EVs, the levels of integrins β1 and α5 on the VSMC surfaces were increased in a time-dependent manner, with a significant increase after 1 hour. Ultimately, there were 26.3% and 24.9% increases in integrins β1 and α5, respectively, in VSMCs after 2 hours of treatment (Figure 6B and 6C).

To determine whether the increases in the integrin levels were caused by transport of EVs into the cell or new production by the cell, we measured the integrin levels on the surface of VSMCs after blocking cellular protein expression with cycloheximide. Briefly, VSMCs were preincubated in the presence of cycloheximide (C7698; Sigma-Aldrich) for 12 hours and then treated with EVs prior to the determination of the integrin levels by enzyme-linked immunosorbent assay. Figure 6D and 6E shows that the levels of both integrins β1 and α5 were significantly increased after treatment with EVs. In addition, we performed real-time polymerase chain reaction analysis, which did not detect any changes in the mRNA levels of either integrin β1 or α5 after treatment with EVs for 2 hours (Figure 6F and 6G).

Discussion

Studies over the past 50 years have revealed numerous cellular and molecular mechanisms that occur during the pathogenesis of atherosclerosis. These studies have shown that intercellular communication between intimal cells plays a key role in the development of this disease. EVs have attracted increasing levels of interest from researchers in the context of their newly identified function as mediators of cell-to-cell communication. Numerous studies have revealed key roles of platelet- and endotheliocyte-derived EVs in atherosclerosis. Additional studies have indicated recently

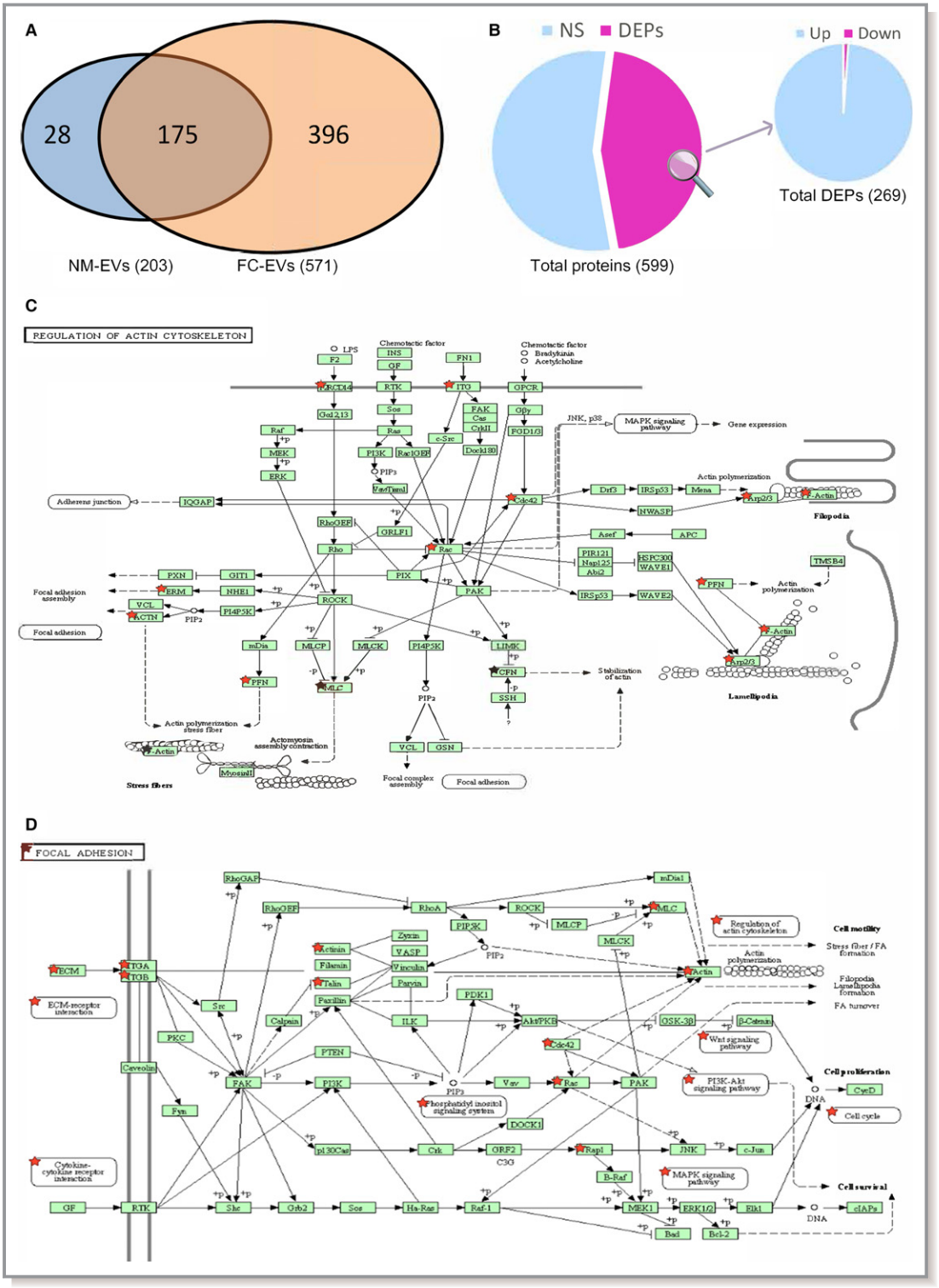

Figure 4. Proteomics analysis of FC-EVs. A, Overview of the proteins detected from NM-EVs and FC-EVs. B, Overview of the DEPs. A DEP is defined as a protein for which there was a significant difference in quantity between the NM-EV and FC-EV groups. "Up" indicates that the quantity of the protein in FC-EVs was greater than in NM-EVs, whereas "Down" indicates lower quantity. C and D, Maps of the "regulation of actin cytoskeleton" and "focal adhesion" pathway analyses of the DEPs, respectively. The "★" symbol in the map means that at least 1 protein detected in the experiment was located at that site of the pathway. DEP indicates differentially expressed protein; FC-EVs, foam cell–derived extracellular vesicles; NM-EVs, normal macrophage–derived extracellular vesicles; NS, not significant; VSMC, vascular smooth muscle cell.

Table 2. The Differentially Expressed Proteins in KEGG Pathway Maps

Uniprot AC	Gene Symbol	Protein Name	P04810	P04510
P60710	ACTB	Actin, cytoplasmic 1	√	√
P57780	ACTN4	α-Actinin 4	√	√
Q9WV32	ARPC1B	Actin-related protein 2/3 complex subunit 1B	√	
P59999	ARPC4	Actin-related protein 2/3 complex subunit 4	√	
Q9CPW4	ARPC5	Actin-related protein 2/3 complex subunit 5	√	
A3KGQ6	ARPC5L	Actin-related protein 2/3 complex subunit 5	√	
P10810	CD14	Monocyte differentiation antigen CD14	√	
P60766	CDC42	Cell division control protein 42 homolog	√	√
P18760	CFL1	Cofilin 1	√	
P08121	COL3A1	Collagen α1(III) chain		√
Q04857	COL6A1	Collagen α1(VI) chain		√
P26040	EZR	Ezrin	√	
Q6ZWQ9	GM6517	MCG5400	√	√
P11688	ITGA5	Integrin α5	√	√
P05555	ITGAM	Integrin αM	√	
P09055	ITGB1	Integrin β1	√	√
Q542I8	ITGB2	Integrin β2	√	
P26041	MSN	Moesin	√	
P62962	PFN1	Profilin 1	√	
P63001	RAC1	Ras-related C3 botulinum toxin substrate 1	√	√
Q05144	RAC2	Ras-related C3 botulinum toxin substrate 2	√	√
Q99JI6	RAP1B	Ras-related protein Rap-1b		√
P26039	TLN1	Talin 1		√

P04810 refers to the KEGG pathway of regulation of actin cytoskeleton; P04510 refers to the KEGG pathway of focal adhesion. The "√" symbol represents the DEP participants in this pathway. KEGG indicates Kyoto Encyclopedia of Genes and Genomes.

that leukocyte- and macrophage-derived EVs from both the circulating blood and atherosclerotic plaques are also involved in the progression of atherosclerosis[29,41,42]; however, the specific roles and detailed information of these macrophage-derived EVs have not yet been fully described. Our study indicated, for the first time, that foam cells could release a higher number of EVs compared with normal macrophages and that these EVs were able to promote VSMC migration and adhesion. These results suggested that reducing foam cell formation with the goal of further reducing the production of EVs may represent a therapeutic option to suppress atherosclerotic vascular disorders.

Macrophages and VSMCs are major players in the pathogenesis of atherosclerotic vascular diseases. VSMCs often reside in vascular lesions close to macrophage clusters and are very likely to be influenced by factors released from proinflammatory cells.[43] Morisaki et al reported that macrophages could accelerate VSMC growth by secreting platelet-derived growth factor.[44] Zhu et at reported that macrophage-derived factors, most likely interleukin 6 and/or tumor necrosis factor α, can enhance the production of matrix metalloproteinase 1 in VSMCs.[45] These studies provided important evidence for potential crosstalk between macrophages and VSMCs; however, the focus of these studies was only on soluble factors, which could not clearly explain some phenomena, such as phenotypic switching of intimal VSMCs during the progression of atherosclerosis. The present study indicated that macrophages in arteriosclerotic lesions may affect VSMCs via EVs and thus induce VSMC migration into and adhesion to the intima. In addition, EVs can be taken up and can release their contents into VSMCs, which may be a mechanism that could account for the phenotypic switching of VSMCs. EVs could easily transfer receptors between cells, and several studies have indicated that EVs play a key role in cell phenotype switch. Specifically, Fogli et al showed that monocyte-derived MPs induced inflammatory and functional alterations in human bronchial smooth muscle cells.[46] These results suggest that EVs may participate in atherogenesis and

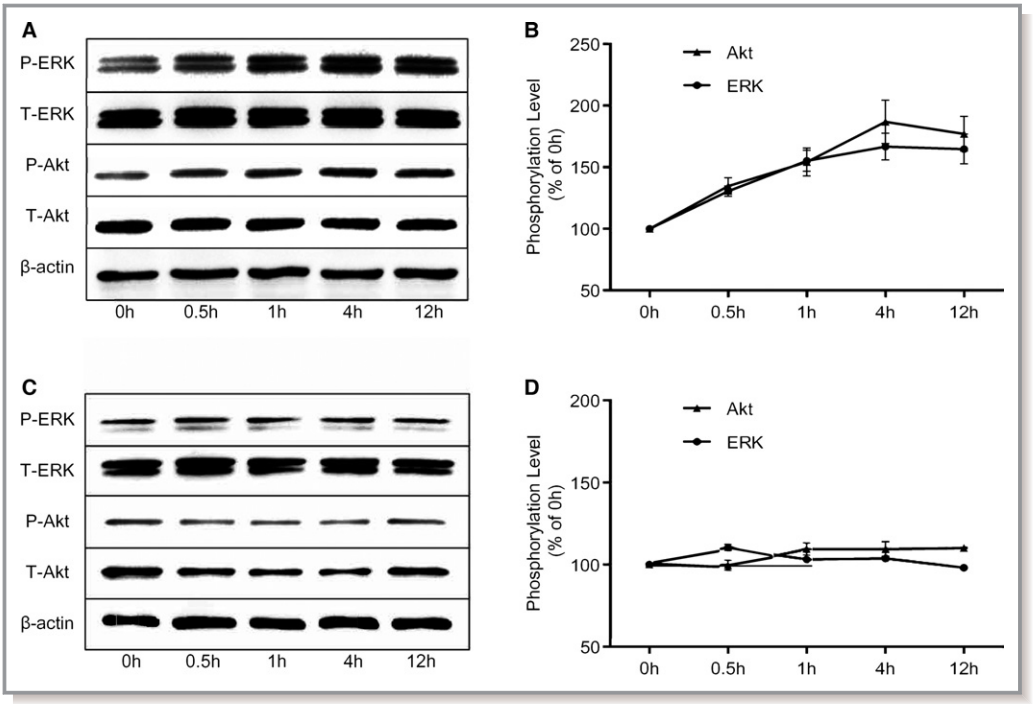

Figure 5. FC-EVs activate the ERK and Akt pathways. A, A representative Western blot result of the phosphorylated forms of ERK and Akt and the total ERK and Akt from VSMCs that had been treated with FC-EVs for the indicated time. B, The line graph of the results of the Western blot. The phosphorylation level was calculated as the ratio of the integrated optical density value of the phosphorylated protein to that of corresponding total protein. C and D, The results of the Western blot for VSMCs treated with the normal macrophage–derived EVs. FC-EVs indicates foam cell–derived extracellular vesicles; P, phosphorylated; T, total; VSMC, vascular smooth muscle cell.

that the roles of EVs in macrophage–VSMC crosstalk during the progression of this disease are worthy of attention.

The growing interest in EVs has led to an exponential increase in the number of publications in the past 20 years.[13] Nevertheless, the isolation, evaluation, classification, identification, and quantitation of EVs are still challenging. In this study, we isolated EVs using ultracentrifugation at 100 000*g*, which did not distinguish between microparticles and exosomes. These EV particles were evaluated using electron microscopy and dynamic light scattering, which are the best methods for identifying EVs. We analyzed the shapes of EVs using a JEM-1400 plus transmission electron microscope and the diameter distribution of EVs using a Delsa Nano C particle analyzer and verified the presence of EVs; however, we did not find significant differences between NM-EVs and FC-EVs (or between circulating EVs from atherosclerotic and health participants) (Figure 2B and 2C and Figure S4). Flow cytometry is by far the best way to characterize and quantify EVs. Nevertheless, the small size of these particles, their heterogeneous cellular origins, the different types of EVs in the mixtures, and a lack of knowledge about EV characterization make it extremely difficult to establish a perfect flow cytometric analysis method for the evaluation of EVs. As in this study (Figures 1E, 1F and 2G, 2H), the relative changes in the numbers of PS- and CD45-positive EVs were different and also differed from changes in the protein level. It is not clear whether these discrepancies were due to the flow cytometry analysis method or the characterization of the EVs. Despite these issues, the fact that the same trends were represented by all 3 measures in our study suggested that our analysis methods were acceptable.

As described previously, EVs may play a role in intercellular communication by acting as signaling complexes that directly stimulate target cells, transfer receptors between cells, deliver proteins to the target cells, and mediate a horizontal transfer of genetic information.[47] It is obvious that the composition of EVs drives these effects. This study revealed, for the first time, the proteome of the NM-EVs and FC-EVs. Meanwhile, the work reported demonstrated that FC-EVs can stimulate the migration and adhesion of VSMCs as well as transfer integrins (receptors for fibronectin and laminin) to the surface of VSMCs and activate pathways in the cell. Our current work, however, focused only on the protein composition of EVs; it has been reported that the microRNA and mRNA species contained in EVs also play important roles in various biological processes.[48–51] The genetic information

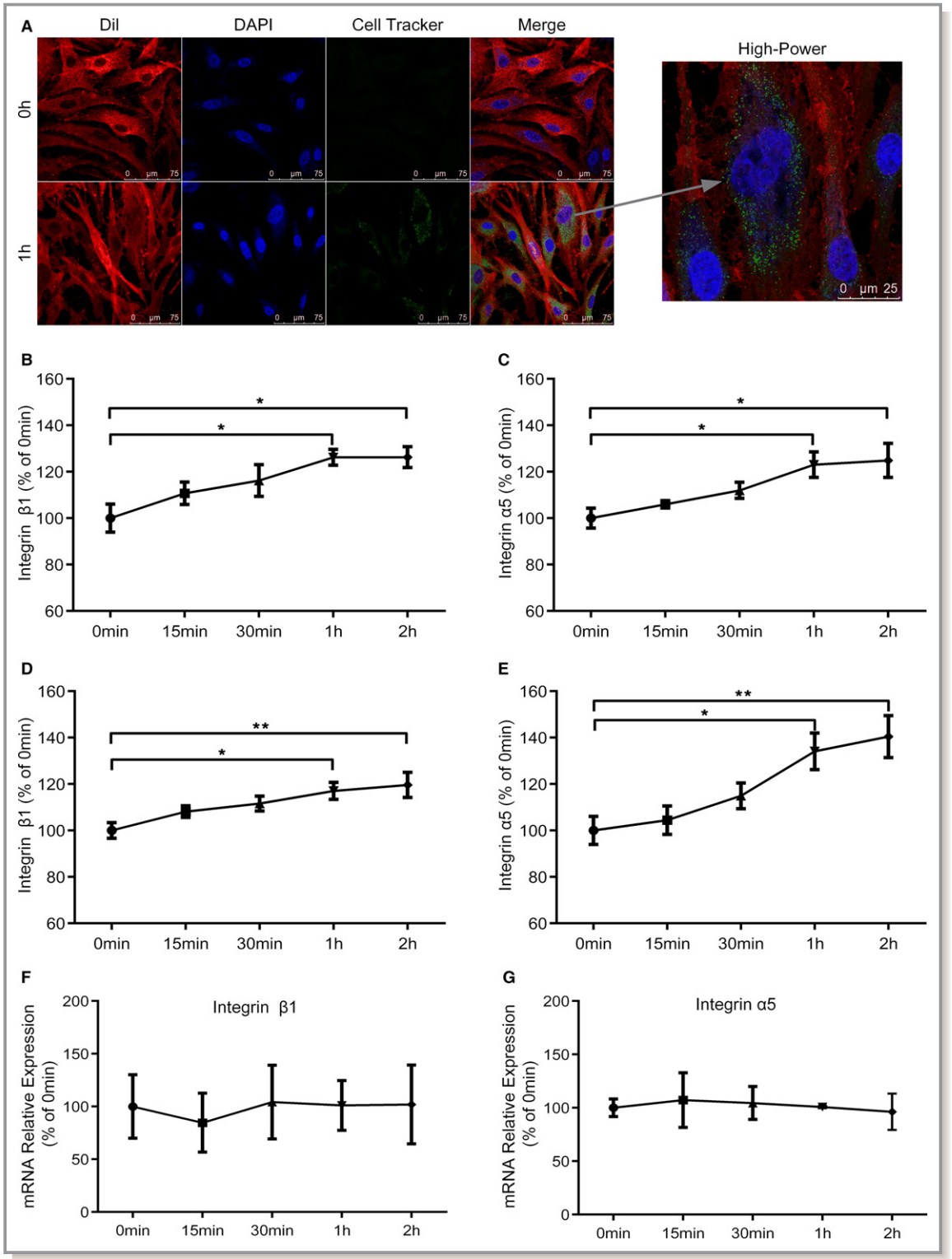

Figure 6. FC-EVs influence VSMCs by conveying proteins. A, The result of confocal microscopy of VSMCs. VSMCs were stained with fluorescent dyes (red DiI for the lipid membranes and blue DAPI for the nuclei) and preincubated with FC-EVs that had been labeled with CellTracker (green). B and C, The protein levels of integrins β1 and α5, respectively, on the surfaces of VSMCs after treatment with FC-EVs for the indicated time, as indicated by the cell enzyme-linked immunosorbent assay experiments. D and E, The protein levels of integrins β1 and α5 on surfaces of VSMCs following treatment with FC-EVs after the protein expression in VSMCs was blocked with cycloheximide. F and G, The results of the real-time polymerase chain reaction analyses for the mRNA levels for integrin β1 and α5 in VSMCs after treatment with FC-EVs for the indicated time. **P*<0.05, ***P*<0.01. FC-EVs indicates foam cell–derived extracellular vesicles; VSMC, vascular smooth muscle cell.

contained in macrophage-derived EVs may be of future interest.

It is well known that integrins are a class of adhesion molecules and are highly organized plasma membrane proteins that establish close connections with the cytoskeleton. Consequently, it is unlikely that integrins are released from the donor cells to target cells in a manner similar to that of cytokines. Nevertheless, EVs generated by exocytosis or budding from cells provide a possible mechanism for the transfer of integrins between cells. In addition, the presence of integrins in EVs was reported in a previous study[40] and was confirmed by our study. In this study, we revealed that FC-EVs can release integrins to the surface of VSMCs. Because integrins can adhere to extracellular matrix components, such as fibronectin, and subsequently activate migration- and adhesion-related pathways in cells, the transfer of integrins from foam cells to VSMCs by EVs might be a potential mechanism for the promotion of VSMC migration and adhesion.

It should be noted that this study had several limitations. First, the mouse-originated J774a.1 foam cells were used throughout the study, although it was more persuasive to use human monocyte–derived foam cells such as THP-1. This choice was made mostly because we have encountered a lot of technical problems when analyzing the characteristic of EVs from suspended THP-1 cells at the early stage of study; we replaced THP-1 with J774a.1 cells and performed most of our experiments. Nevertheless, we also used EVs from THP-1 and U937 foam cells to perform the key biological experiments and to verify the results obtained using J774a.1 cells. The another limitation was that the sample used for proteomic analysis was very small (only 2 biological duplicates by 2 technical duplicates). Unlike biological experiments, proteomic analysis, as a high-throughput technique, is difficult to use for drawing firm conclusions, so it is usually applied to exploratory study. The proteomic analysis in this study was exploratory. Even so, the results of proteomic analysis were interesting and worthy of further study. All of the identified proteins and their quantitative results are shown in Table S1. The third limitation was that because no effective methods exist to acquire pure microparticles without exosomes, like many other studies, this study focused on whole EVs instead of a single type of microparticles or exosomes. It would be interesting to determine the percentage of exosomes and microparticles present in EVs, to clarify the functions of exosomes and microparticles, and to further describe which type of EV plays a predominant role in changing the VSMC capacity for migration and adhesion.

In summary, this study demonstrated for the first time that macrophage-derived foam cells release more EVs than normal macrophages and that FC-EVs are capable of transporting proteins to VSMCs, thus activating the ERK and Akt pathways in VSMCs and promoting VSMC migration and adhesion. These data suggest that EV-mediated intercellular communication might be important in the progression of atherosclerosis.

Sources of Funding

This project was supported by Grant 2011CB503900 from "973" National S&T Major Project; by Grant 81370235, 81170101 from the National Natural Science Foundation of China; Grant 7122106 from the Natural Science Foundation of Beijing, and by 1S10RR031537-01 from the NIH.

Disclosures

None.

References

1. Pan BT, Teng K, Wu C, Adam M, Johnstone RM. Electron microscopic evidence for externalization of the transferrin receptor in vesicular form in sheep reticulocytes. *J Cell Biol*. 1985;101:942–948.
2. Heijnen HF, Schiel AE, Fijnheer R, Geuze HJ, Sixma JJ. Activated platelets release two types of membrane vesicles: microvesicles by surface shedding and exosomes derived from exocytosis of multivesicular bodies and alpha-granules. *Blood*. 1999;94:3791–3799.
3. Taraboletti G, D'Ascenzo S, Borsotti P, Giavazzi R, Pavan A, Dolo V. Shedding of the matrix metalloproteinases MMP-2, MMP-9, and MT1-MMP as membrane vesicle-associated components by endothelial cells. *Am J Pathol*. 2002;160:673–680.
4. EL Andaloussi S, Mager I, Breakefield XO, Wood MJ. Extracellular vesicles: biology and emerging therapeutic opportunities. *Nat Rev Drug Discov*. 2013;12:347–357.
5. Faure J, Lachenal G, Court M, Hirrlinger J, Chatellard-Causse C, Blot B, Grange J, Schoehn G, Goldberg Y, Boyer V, Kirchhoff F, Raposo G, Garin J, Sadoul R. Exosomes are released by cultured cortical neurones. *Mol Cell Neurosci*. 2006;31:642–648.
6. Al-Nedawi K, Meehan B, Kerbel RS, Allison AC, Rak J. Endothelial expression of autocrine VEGF upon the uptake of tumor-derived microvesicles containing oncogenic EGFR. *Proc Natl Acad Sci USA*. 2009;106:3794–3799.
7. Zomer A, Vendrig T, Hopmans ES, van Eijndhoven M, Middeldorp JM, Pegtel DM. Exosomes: fit to deliver small RNA. *Commun Integr Biol*. 2010;3:447–450.
8. Raposo G, Stoorvogel W. Extracellular vesicles: exosomes, microvesicles, and friends. *J Cell Biol*. 2013;200:373–383.
9. Ashcroft BA, de Sonneville J, Yuana Y, Osanto S, Bertina R, Kuil ME, Oosterkamp TH. Determination of the size distribution of blood microparticles directly in plasma using atomic force microscopy and microfluidics. *Biomed Microdevices*. 2012;14:641–649.
10. Raposo G, Nijman HW, Stoorvogel W, Liejendekker R, Harding CV, Melief CJ, Geuze HJ. B lymphocytes secrete antigen-presenting vesicles. *J Exp Med*. 1996;183:1161–1172.
11. van der Pol E, Boing AN, Harrison P, Sturk A, Nieuwland R. Classification, functions, and clinical relevance of extracellular vesicles. *Pharmacol Rev*. 2012;64:676–705.
12. Yuana Y, Sturk A, Nieuwland R. Extracellular vesicles in physiological and pathological conditions. *Blood Rev*. 2013;27:31–39.
13. Loyer X, Vion AC, Tedgui A, Boulanger CM. Microvesicles as cell-cell messengers in cardiovascular diseases. *Circ Res*. 2014;114:345–353.
14. Ratajczak J, Miekus K, Kucia M, Zhang J, Reca R, Dvorak P, Ratajczak MZ. Embryonic stem cell-derived microvesicles reprogram hematopoietic progenitors: evidence for horizontal transfer of mRNA and protein delivery. *Leukemia*. 2006;20:847–856.
15. Gatti S, Bruno S, Deregibus MC, Sordi A, Cantaluppi V, Tetta C, Camussi G. Microvesicles derived from human adult mesenchymal stem cells protect against ischaemia-reperfusion-induced acute and chronic kidney injury. *Nephrol Dial Transplant*. 2011;26:1474–1483.

16. Del Conde I, Shrimpton CN, Thiagarajan P, Lopez JA. Tissue-factor-bearing microvesicles arise from lipid rafts and fuse with activated platelets to initiate coagulation. *Blood*. 2005;106:1604–1611.
17. Camussi G, Deregibus MC, Bruno S, Grange C, Fonsato V, Tetta C. Exosome/microvesicle-mediated epigenetic reprogramming of cells. *Am J Cancer Res*. 2011;1:98–110.
18. Rak J, Guha A. Extracellular vesicles—vehicles that spread cancer genes. *Bioessays*. 2012;34:489–497.
19. Fevrier B, Vilette D, Archer F, Loew D, Faigle W, Vidal M, Laude H, Raposo G. Cells release prions in association with exosomes. *Proc Natl Acad Sci USA*. 2004;101:9683–9688.
20. Rajendran L, Honsho M, Zahn TR, Keller P, Geiger KD, Verkade P, Simons K. Alzheimer's disease beta-amyloid peptides are released in association with exosomes. *Proc Natl Acad Sci USA*. 2006;103:11172–11177.
21. Emmanouilidou E, Melachroinou K, Roumeliotis T, Garbis SD, Ntzouni M, Margaritis LH, Stefanis L, Vekrellis K. Cell-produced alpha-synuclein is secreted in a calcium-dependent manner by exosomes and impacts neuronal survival. *J Neurosci*. 2010;30:6838–6851.
22. Bang C, Batkai S, Dangwal S, Gupta SK, Foinquinos A, Holzmann A, Just A, Remke J, Zimmer K, Zeug A, Ponimaskin E, Schmiedl A, Yin X, Mayr M, Halder R, Fischer A, Engelhardt S, Wei Y, Schober A, Fiedler J, Thum T. Cardiac fibroblast-derived microRNA passenger strand-enriched exosomes mediate cardiomyocyte hypertrophy. *J Clin Invest*. 2014;124:2136–2146.
23. Waldenstrom A, Ronquist G. Role of exosomes in myocardial remodeling. *Circ Res*. 2014;114:315–324.
24. Condorelli G, Latronico MV, Cavarretta E. Micrornas in cardiovascular diseases: current knowledge and the road ahead. *J Am Coll Cardiol*. 2014;63:2177–2187.
25. Schiro A, Wilkinson FL, Weston R, Smyth JV, Serracino-Inglott F, Alexander MY. Endothelial microparticles as conveyors of information in atherosclerotic disease. *Atherosclerosis*. 2014;234:295–302.
26. Go AS, Mozaffarian D, Roger VL, Benjamin EJ, Berry JD, Blaha MJ, Dai S, Ford ES, Fox CS, Franco S, Fullerton HJ, Gillespie C, Hailpern SM, Heit JA, Howard VJ, Huffman MD, Judd SE, Kissela BM, Kittner SJ, Lackland DT, Lichtman JH, Lisabeth LD, Mackey RH, Magid DJ, Marcus GM, Marelli A, Matchar DB, McGuire DK, Mohler ER III, Moy CS, Mussolino ME, Neumar RW, Nichol G, Pandey DK, Paynter NP, Reeves MJ, Sorlie PD, Stein J, Towfighi A, Turan TN, Virani SS, Wong ND, Woo D, Turner MB; American Heart Association Statistics C, Stroke Statistics S. Executive summary: heart disease and stroke statistics—2014 update: a report from the American Heart Association. *Circulation*. 2014;129:399–410.
27. Lusis AJ. Atherosclerosis. *Nature*. 2000;407:233–241.
28. Helal O, Defoort C, Robert S, Marin C, Lesavre N, Lopez-Miranda J, Riserus U, Basu S, Lovegrove J, McMonagle J, Roche HM, Dignat-George F, Lairon D. Increased levels of microparticles originating from endothelial cells, platelets and erythrocytes in subjects with metabolic syndrome: relationship with oxidative stress. *Nutr Metab Cardiovasc Dis*. 2011;21:665–671.
29. Sarlon-Bartoli G, Bennis Y, Lacroix R, Piercecchi-Marti MD, Bartoli MA, Arnaud L, Mancini J, Boudes A, Sarlon E, Thevenin B, Leroyer AS, Squarcioni C, Magnan PE, Dignat-George F, Sabatier F. Plasmatic level of leukocyte-derived microparticles is associated with unstable plaque in asymptomatic patients with high-grade carotid stenosis. *J Am Coll Cardiol*. 2013;62:1436–1441.
30. Rautou PE, Vion AC, Amabile N, Chironi G, Simon A, Tedgui A, Boulanger CM. Microparticles, vascular function, and atherothrombosis. *Circ Res*. 2011;109:593–606.
31. Sanborn MR, Thom SR, Bohman LE, Stein SC, Levine JM, Milovanova T, Maloney-Wilensky E, Frangos S, Kumar MA. Temporal dynamics of microparticle elevation following subarachnoid hemorrhage. *J Neurosurg*. 2012;117:579–586.
32. Omoto S, Nomura S, Shouzu A, Nishikawa M, Fukuhara S, Iwasaka T. Detection of monocyte-derived microparticles in patients with type II diabetes mellitus. *Diabetologia*. 2002;45:550–555.
33. Haqqani AS, Delaney CE, Tremblay TL, Sodja C, Sandhu JK, Stanimirovic DB. Method for isolation and molecular characterization of extracellular microvesicles released from brain endothelial cells. *Fluids Barriers CNS*. 2013;10:4.
34. Ratheesh A, Ingle A, Gude RP. Pentoxifylline modulates cell surface integrin expression and integrin mediated adhesion of B16F10 cells to extracellular matrix components. *Cancer Biol Ther*. 2007;6:1743–1752.
35. Robert S, Poncelet P, Lacroix R, Arnaud L, Giraudo L, Hauchard A, Sampol J, Dignat-George F. Standardization of platelet-derived microparticle counting using calibrated beads and a Cytomics FC500 routine flow cytometer: a first step towards multicenter studies? *J Thromb Haemost*. 2009;7:190–197.
36. Shan LY, Li JZ, Zu LY, Niu CG, Ferro A, Zhang YD, Zheng LM, Ji Y. Platelet-derived microparticles are implicated in remote ischemia conditioning in a rat model of cerebral infarction. *CNS Neurosci Ther*. 2013;19:917–925.
37. Robert S, Lacroix R, Poncelet P, Harhouri K, Bouriche T, Judicone C, Wischhusen J, Arnaud L, Dignat-George F. High-sensitivity flow cytometry provides access to standardized measurement of small-size microparticles—brief report. *Arterioscler Thromb Vasc Biol*. 2012;32:1054–1058.
38. Ross R. Atherosclerosis is an inflammatory disease. *Am Heart J*. 1999;138:S419–S420.
39. Gyorgy B, Modos K, Pallinger E, Paloczi K, Pasztoi M, Misjak P, Deli MA, Sipos A, Szalai A, Voszka I, Polgar A, Toth K, Csete M, Nagy G, Gay S, Falus A, Kittel A, Buzas EI. Detection and isolation of cell-derived microparticles are compromised by protein complexes resulting from shared biophysical parameters. *Blood*. 2011;117:e39–e48.
40. Thery C, Ostrowski M, Segura E. Membrane vesicles as conveyors of immune responses. *Nat Rev Immunol*. 2009;9:581–593.
41. Leroyer AS, Isobe H, Leseche G, Castier Y, Wassef M, Mallat Z, Binder BR, Tedgui A, Boulanger CM. Cellular origins and thrombogenic activity of microparticles isolated from human atherosclerotic plaques. *J Am Coll Cardiol*. 2007;49:772–777.
42. Rautou PE, Leroyer AS, Ramkhelawon B, Devue C, Duflaut D, Vion AC, Nalbone G, Castier Y, Leseche G, Lehoux S, Tedgui A, Boulanger CM. Microparticles from human atherosclerotic plaques promote endothelial ICAM-1-dependent monocyte adhesion and transendothelial migration. *Circ Res*. 2011;108:335–343.
43. Koga J, Aikawa M. Crosstalk between macrophages and smooth muscle cells in atherosclerotic vascular diseases. *Vascul Pharmacol*. 2012;57:24–28.
44. Morisaki N, Koyama N, Kawano M, Mori S, Umemiya K, Koshikawa T, Saito Y, Yoshida S. Human macrophages modulate the phenotype of cultured rabbit aortic smooth muscle cells through secretion of platelet-derived growth factor. *Eur J Clin Invest*. 1992;22:461–468.
45. Zhu Y, Hojo Y, Ikeda U, Takahashi M, Shimada K. Interaction between monocytes and vascular smooth muscle cells enhances matrix metalloproteinase-1 production. *J Cardiovasc Pharmacol*. 2000;36:152–161.
46. Fogli S, Stefanelli F, Neri T, Bardelli C, Amoruso A, Brunelleschi S, Celi A, Breschi MC. Montelukast prevents microparticle-induced inflammatory and functional alterations in human bronchial smooth muscle cells. *Pharmacol Res*. 2013;76:149–156.
47. Camussi G, Deregibus MC, Bruno S, Cantaluppi V, Biancone L. Exosomes/microvesicles as a mechanism of cell-to-cell communication. *Kidney Int*. 2010;78:838–848.
48. Fernandez-Messina L, Gutierrez-Vazquez C, Rivas-Garcia E, Sanchez-Madrid F, de la Fuente H. Immunomodulatory role of microRNAs transferred by extracellular vesicles. *Biol Cell*. 2015;107:61–77.
49. Penfornis P, Vallabhaneni KC, Whitt J, Pochampally R. Extracellular vesicles as carriers of microRNA, proteins and lipids in tumor microenvironment. *Int J Cancer*. 2016;138:14–21.
50. Jansen F, Yang X, Hoelscher M, Cattelan A, Schmitz T, Proebsting S, Wenzel D, Vosen S, Franklin BS, Fleischmann BK, Nickenig G, Werner N. Endothelial microparticle-mediated transfer of microRNA-126 promotes vascular endothelial cell repair via SPRED1 and is abrogated in glucose-damaged endothelial microparticles. *Circulation*. 2013;128:2026–2038.
51. Li J, Zhang Y, Liu Y, Dai X, Li W, Cai X, Yin Y, Wang Q, Xue Y, Wang C, Li D, Hou D, Jiang X, Zhang J, Zen K, Chen X, Zhang CY. Microvesicle-mediated transfer of microRNA-150 from monocytes to endothelial cells promotes angiogenesis. *J Biol Chem*. 2013;288:23586–23596.

SUPPLEMENTAL MATERIAL

Figure S1

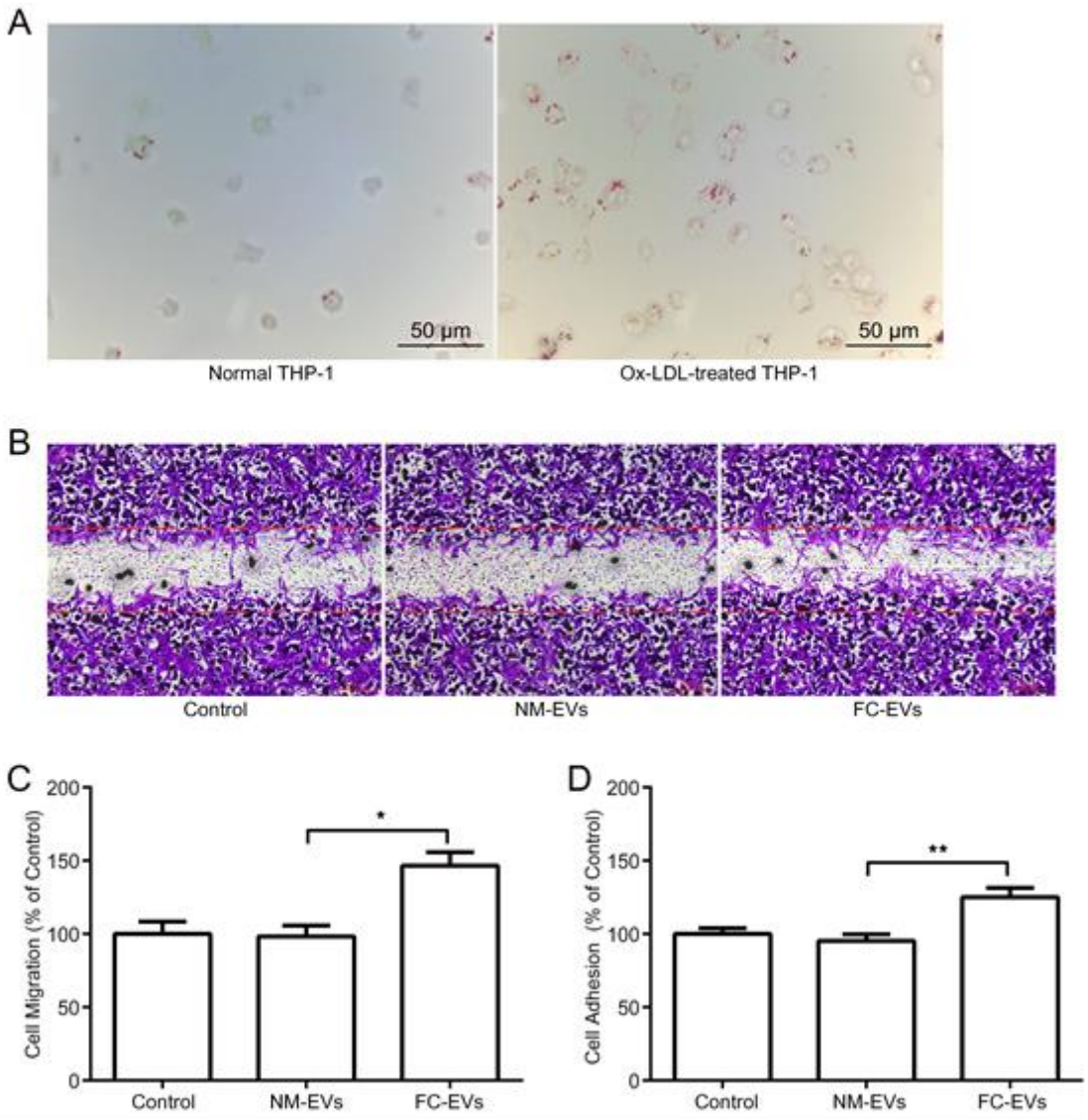

THP-1 foam cell-derived EVs promote VSMC migration and adhesion. Control, NM-EVs, FC-EVs in this figure refer to the untreated group and those treated with normal macrophage-derived EVs and foam cell-derived EVs, respectively. (A) shows foam cell formation for THP-1 cells. (B-D) are the data for wound healing and cell adhesion assays on VSMCs after indicated treatment. (B) is the representative photograph of VSMC migration in wound healing assay. (C) is the quantification for VSMC migration. (D) is the result of VSMC adhesion experiments.

Figure S2

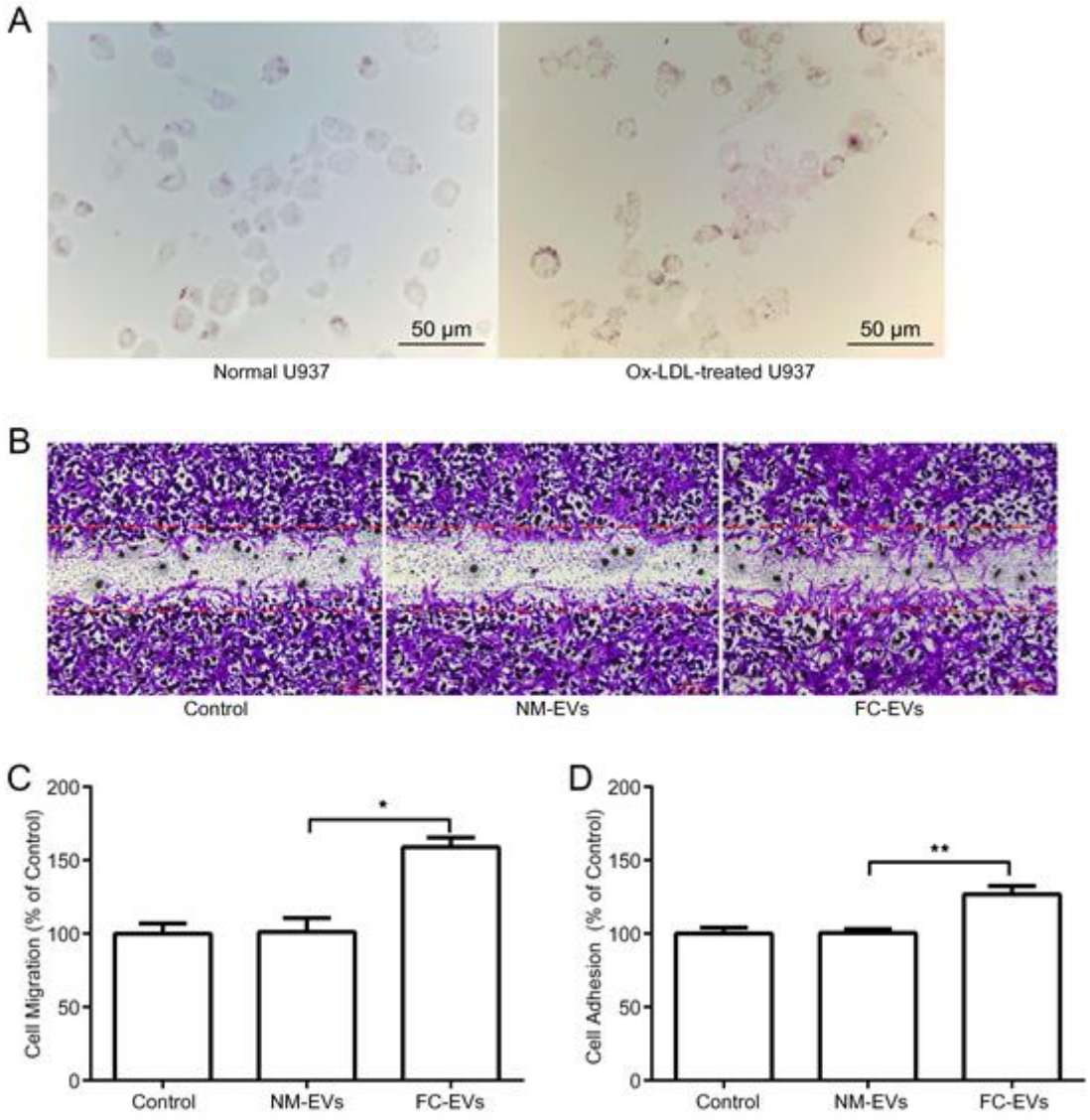

U937 foam cell-derived EVs promote VSMC migration and adhesion. Control, NM-EVs, FC-EVs in this figure refer to the untreated group and those treated with normal macrophage-derived EVs and foam cell-derived EVs, respectively. (A) shows foam cell formation for U937 cells. (B-D) are the data for wound healing and cell adhesion assays on VSMCs after indicated treatment. (B) is the representative photograph of VSMC migration in wound healing assay. (C) is the quantification for VSMC migration. (D) is the result of VSMC adhesion experiments.

Figure S3

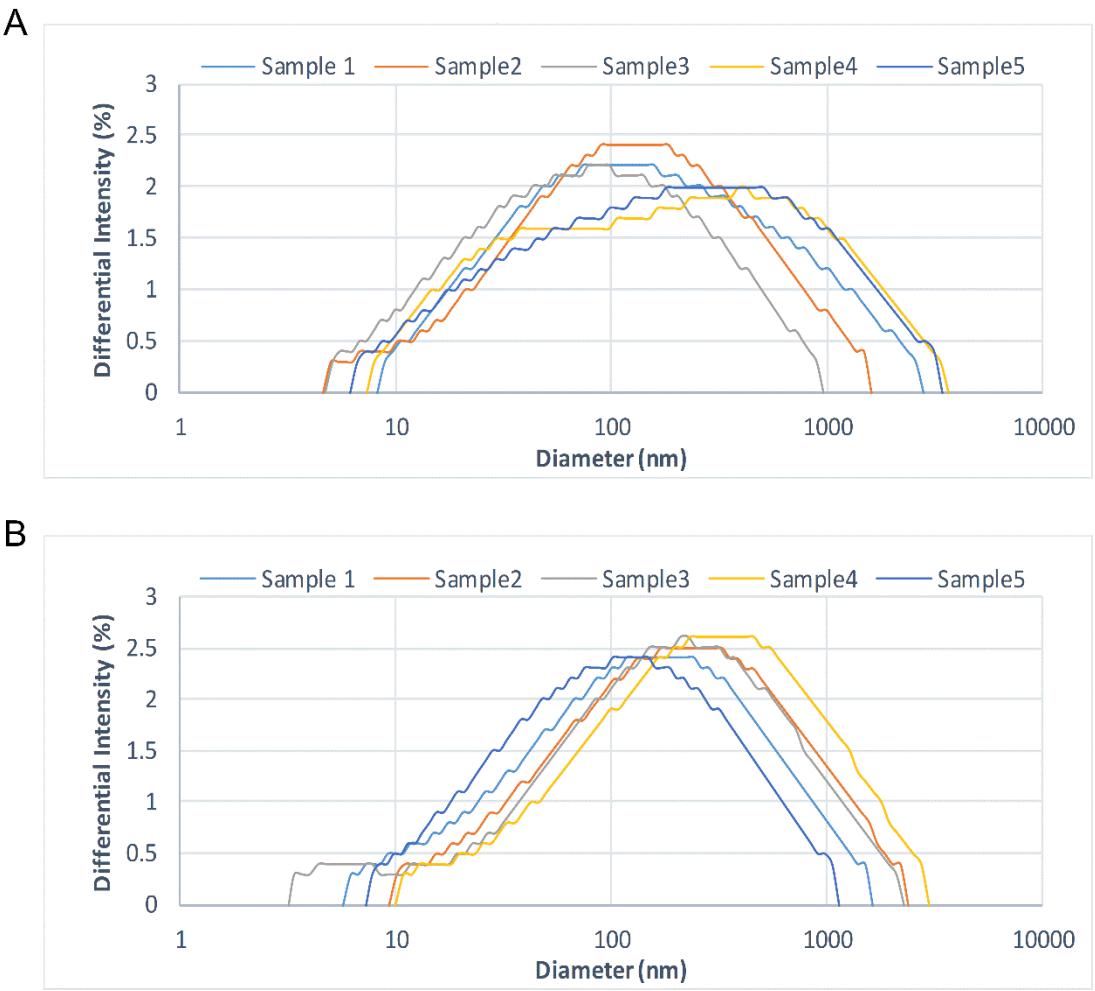

Nanoparticle analysis for plasma from atherosclerotic subjects and healthy subjects by dynamic light scattering. (A) shows the intensity distributions of particles with different diameters, which were from 5 atherosclerotic subjects. (B) shows the intensity distributions of particles with different diameters from 5 healthy subjects.

Figure S4

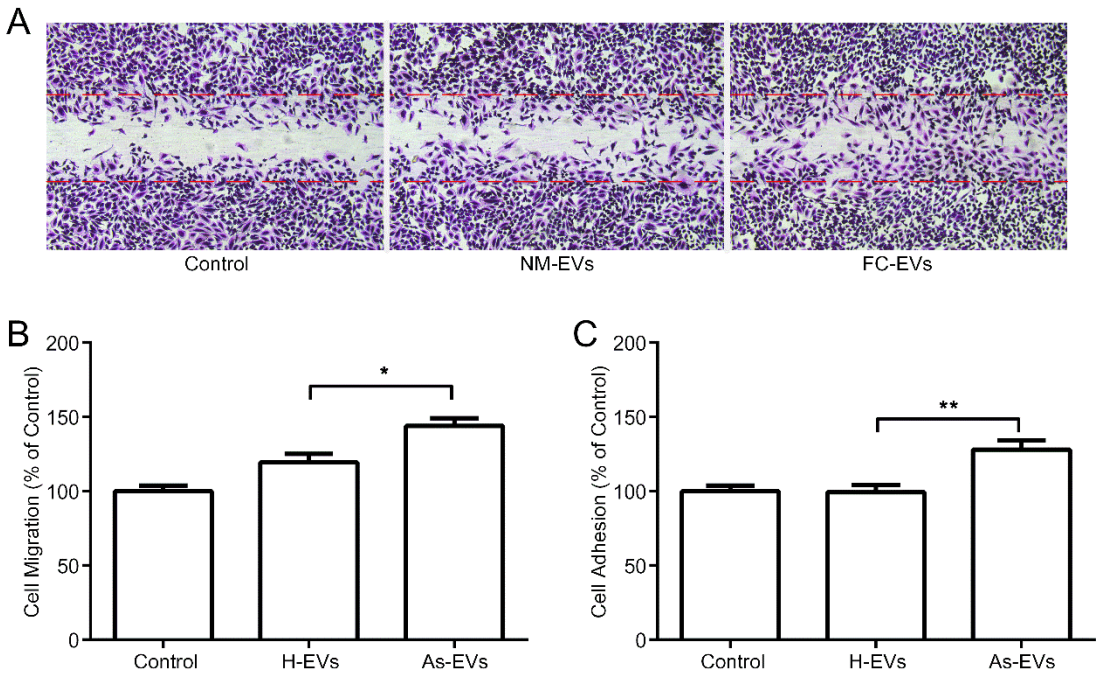

J774a.1 foam cell-derived EVs promote HUVEC migration and adhesion. Control, NM-EVs, FC-EVs in this figure refer to the untreated group and those treated with normal macrophage-derived EVs and foam cell-derived EVs, respectively. This figure shows the data for wound healing and cell adhesion assays on HUVECs (Human umbilical vein endothelial cells) after indicated treatment. (A) is the representative photograph of HUVEC migration in wound healing assay. (B) is the quantification for HUVEC migration. (C) is the result of HUVEC adhesion experiments.